Energy, Mines and Resources Canada | Énergie, Mines et Ressources Canada

CANMET

Canada Centre for Mineral and Energy Technology | Centre canadien de la technologie des minéraux et de l'énergie

MINERALOGICAL AND IMAGE ANALYSIS STUDY OF SAMPLES FROM CORE WA20 OF THE WAITE AMULET TAILINGS

W. Petruk and R.G. Pinard
Mineral Processing Laboratory

June 1986

MICROMEDIA

This document is an interim report prepared ... to ... report ... represent ... the opinion ... for Mineral ... (CANMET)

... rapport ... rapport ... de ... recommandations ... définitive de ... Centre canadien de ... minéraux et de l'énergie (CANMET)

Project: 30.86.02
Tailings Management

23 pp

MINERAL SCIENCES LABORATORIES
DIVISION REPORT MSL 86-87 (IR)

MINERALOGICAL AND IMAGE ANALYSIS STUDY OF SAMPLES FROM CORE WA20 OF THE WAITE AMULET TAILINGS

by

W. Petruk and R.G. Pinard

ABSTRACT

A study was conducted on a suite of samples from different horizons of the Waite Amulet tailings pile to determine the mineralogical characteristics and mineral alterations that have occurred since the tailings were deposited. Data on mineral quantities show that the tailings contain about 60 wt % pyrite and 14 wt % pyrrhotite at 1 m below the water table; about 25 wt % pyrite and 6 wt % pyrrhotite at the water table; about 5 wt % pyrite and 5 wt % pyrrhotite in the unsaturated zone; both minerals are absent in the near surface zone. These data indicate that alteration of sulphide minerals progresses slowly below the water table, faster in the unsaturated zone, and has been completed near surface. The mineral associations provide evidence for the sequential replacement of pyrrhotite but not of pyrite. In particular, the pyrrhotite is transformed from the grain edges towards grain centres to phases which contain various amounts of iron sulphate and water. These phases are in turn converted to a sulphur-rich "goethite". On the other hand, pyrite appears to have altered directly to "goethite".

ÉTUDE MINÉRALOGIQUE ET ANALYSE D'IMAGE DES ÉCHANTILLONS PROVENANT DU CAROTTAGE WA20 DES RÉSIDUS DE WAITE AMULET

par

W. Petruck et R.G. Pinard

RÉSUMÉ

On a fait l'étude d'une gamme d'échantillons recueillis à différents horizons de l'amas de résidus de Waite Amulet en vue de déterminer les caractéristiques minéralogiques et les altérations minérales qui se sont produites depuis que les résidus ont été déposés. Les données relatives aux quantités minérales indiquent que les résidus qui se trouvent à 1 m sous la nappe phréatique ont une teneur en pyrite d'environ 60 % (en poids) et 14 % (en poids) en pyrrhotine; une teneur en pyrite d'environ 25 % (en poids) et 6 % (en poids) en pyrrhotine au niveau de la nappe phréatique; une teneur en pyrite d'environ 5 % (en poids) et 5% (en poids) en pyrrhotine dans la zone non saturée; et que les deux minéraux sont absents près de la surface du sol. Ces données indiquent que l'altération des minéraux sulfurés progresse lentement dans les couches situées sous la nappe phréatique, plus rapidement dans la zone non saturée et qu'elle est totale dans les zones près de la surface. Les minéraux associés font la preuve du remplacement séquentiel de la pyrrhotine mais non de la pyrite. La pyrrhotine, en particulier, est transformée en phases FeS_2 à partir des points intergranulaires vers le centre granulaire. Ces phases sont, à leur tour, changées en "goethite" à haute teneur en soufre. D'autre part, la pyrite semble s'être altérée directement en "goéthite".

INTRODUCTION

A hydrogeochemical investigation is being conducted on the Waite Amulet tailings by Noranda Research Centre and CANMET as part of the Joint Industry/CANMET Reactive Acid Tailings Program. The Waite Amulet tailings area is situated about 20 kilometres north of Noranda, Quebec and contains about 6.5 million tonnes of reactive sulphide tailings. The tailings were deposited prior to 1962 and were successfully vegetated in 1978 and 1979. Lush vegetation covers the tailings pile, but acid seepages are found at the base. The acid is collected in an acid water resevoir and treated in a treatment plant. The objective of the investigation is to determine the biohydrogeochemical processes and controlling mechanisms, in order to develop a long term tailings management program which would eliminate the need for perpetual maintenance and water treatment at the Waite Amulet tailings site, and to develop a model that may be applicable to other tailings.

The study was begun by Noranda Research Centre in September, 1985. They reported that twenty-three piezometer nests were placed, nine cores were taken, the level of the water table was established, pH readings were taken, and bacterial counts were determined for two of the nine cores. They also reported that the pH increases with depth from about 3 to 6 in the unsaturated zone, and is generally greater than 6 below the water table. In addition a strong presence of the sulphur reducing bacteria, thiobacillus ferroxidans, is indicated in the upper 2 metres of the tailings, but the bacteria were not detected below the water table.

A suite of samples from core WA20 (Fig. 1 and 2), taken at 0.3 metre intervals from 0.3 to 3.0 metres below surface, was studied in the Process Mineralogy Section at CANMET to characterize the material. The samples received consisted of unconsolidated material. They were, therefore, screened into plus and minus 37 µm (400 mesh) fractions so that the large grains could be analysed at low power magnification (Table 1). Polished sections were prepared from the screened fractions and studied with the automated MP-SEM-IPS image analysis system. The minerals and phases present were identified with the energy dispersive X-ray analyser (EDXA), the compositions of the alteration products were determined by quantitative analysis with the EDXA, and mineral quantities and the relationships

between the minerals and alteration products were determined with the image analyser.

GENERAL MINERALOGY

The minerals and phases found in the samples are silicates, sulphides, oxides, sulphates and carbonates. The main silicate minerals are quartz, orthoclase, amphibole and/or pyroxene, and chlorite; a minor one is mica. The main sulphide minerals are pyrite and pyrrhotite; minor ones are sphalerite and chalcopyrite; and those in trace amounts are bismuthinite and tetrahedrite. The main oxides are magnetite and goethite, and a minor one is cassiterite. One grain of calcite was found. The sulphates are alteration products of pyrrhotite and pyrite. The main ones are interpreted as $FeSO_4$ with various amounts of FeS_2 and water. In addition a small amount of jarosite was found in samples taken at 0.3 and 1.8 metres. Backscattered electron photographs of the +37 μm (plus 400 mesh) fractions are shown in Fig. 3 to give a pictorial presentation of the mineral distributions in the samples.

ALTERATION PRODUCTS

Pyrrhotite has altered through several stages to a sulphur-rich "goethite", whereas pyrite alters directly to goethite. Alteration of pyrrhotite is evident in all samples taken from 0.6 to 3.0 m but is most pronounced in samples from 1.2 to 2.1 m. The alteration appears as a narrow band around pyrrhotite grains in the sample from 3.0 m, and as wider bands as well as separate particles in samples from closer to surface. By contrast the alteration of pyrite is not apparent in most samples. Data on mineral quantities indicate, however, that pyrite decomposes. Pyrite accounts for about 60 wt % of the material in the sample from 3.0 m, for about 1 to 6 wt % of the material in samples from 0.6 to 1.8 m, and is essentially absent in the sample from 0.3 m.

Pyrrhotite Alteration

At least four types of alteration products were observed on the pyrrhotite particles. The first type (Phase 1) is a phase whose optical properties are similar to those of marcasite, and whose composition is equivalent to FeS_2 (Table 2). This phase surrounds pyrrhotite grains as a band up to 15 micrometres wide (Fig. 4). The second type (Phase 2) also occurs as a band around pyrrhotite grains (Fig. 5). It contains only about 44 wt % Fe and 47 wt % S for a total of 91 wt %, the remainder is assumed to be either oxygen or water since no other elements were indicated by the energy dispersive X-ray (EDXA) spectrum. This composition is equivalent to $7FeS_2 \cdot FeSO_4 \cdot H_2O$; there may be other ways of expressing the composition of this phase. Both phase 1 and 2 contain lamellae (Fig. 6) that probably developed by replacement, along cleavage planes, of pyrrhotite with a hydrous form of $FeSO_4$. Semiquantitative analysis of the lamellae gives a lower total element content than the total for phase 2. Phase 3 has the same texture as phase 2 but the average Fe and S contents are 42 and 44 wt % respectively, for a total of 86 wt % which may be expressed as $2FeS_2 \cdot FeSO_4 \cdot H_2O$. Phase 4 also occurs as bands around pyrrhotite, but it tends to be more massive than phases 1, 2 and 3 (Fig. 7) and contains considerably less sulphur and has a lower Fe plus S total. It contains, in wt %, about Fe 43, S 29, total 72. This composition may be expressed as $FeS_2 \cdot FeSO_4 \cdot H_2O$. The lamellar structure in phases 1, 2 and 3 is retained in some grains that have nearly replaced the pyrrhotite (Fig. 8 and 9) and have compositions that range from the equivalent of $FeS_2 \cdot FeSO_4 \cdot H_2O$ to $FeS_2 \cdot FeSO_4 \cdot 7H_2O$. The apparent end phase of this alteration process is a sulphur-rich "goethite" that contains an average of 38 wt % Fe, 12 wt % S, 1.6 wt % Al and 0.9 wt % Si, for a total of 52 wt % (Table 2) which may be expressed as $FeO \cdot FeSO_4 \cdot 4H_2O$.

Pyrite Alteration

Alteration of pyrite is not readily observed in the samples. However, the quantity of pyrite decreases from about 60 wt % in the sample at 3.0 m to 0.3 wt % in the sample at 0.3 m, which indicates that the alteration products from pyrite have been washed away. The only evidence of pyrite alteration was pyrite remnants in a goethite matrix (Fig. 10). The goethite with pyrite remnants contains 1 to 5 wt % sulphur and small amounts of silicon and aluminium (Table 2).

"Goethite"

The goethite contains less iron than stoichemetric goethite; therefore it is referred to as "goethite". The sulphur-rich "goethite" grains that apparently formed by alteration of pyrrhotite cannot be readily differentiated from the low-sulphur "goethite" grains which probably formed by alteration of pyrite. Therefore, for determination of mineral quantities, both varieties are combined and referred to as "goethite". Both the low- and high-sulphur "goethite" are deposited as borders on all the minerals (Fig. 11, 12 and 13), but the sulphur-rich variety appears to have reacted with magnetite (Fig. 12). Much of the "goethite" in the sample from the near surface zone (Sample 0.3 m) is present as discrete grains (Fig. 14).

Alteration of Chalcopyrite

A trace amount of chalcopyrite is present in all samples but no secondary copper minerals such as covellite or chalcocite were observed.

MINERAL QUANTITIES

Mineral quantities were determined with the image analysis system for both the plus and minus 37 μm (400 mesh) fractions of each sample (Tables 3 and 4). Both sets of data show the same changes from sample to sample. In particular, the pyrite and pyrrhotite contents decrease towards the surface of the tailings pile, but there is no apparent increase in quantity of "goethite" as the quantities of pyrite and pyrrhotite decrease except for the sample from 0.3 m, which contains a high amount of "goethite".

Two types of ternary diagrams were drawn for mineral quantities in the plus and minus 37 μm (400 mesh) fractions to show progressive changes in samples from the base to the surface of the tailings pile. One diagram is a silicate-magnetite-pyrite+pyrrhotite ternary, and the other a pyrite-pyrrhotite-"goethite"+alteration products ternary. The diagrams for both the plus and minus 37 μm (400 mesh) fractions show the same trends (Fig. 15,16,17 and 18). The silicates-magnetite-pyrite+pyrrhotite ternaries show a decrease of pyrite+pyrrhotite towards the magnetite- silicates tie-line, and three zones can be defined by either a grouping of points or a progressive change in point positions. The zones are:

(1) below 2 m (below the water table), (2) 0.6 to 2 m (unsaturated zone), and (3) above 0.6 m (near surface). It is noteworthy that for samples from below the water table the mineralogical proportions of Sample 2.1 m (No. 7) fall between that of Sample 2.7 m (No. 9) and 3.0 m (No. 10). By contrast, the mineralogical composition indicates that Sample 2.4 m (No. 8) is more altered than any other sample from below the water table.

The mineralogical proportions of the samples from the unsaturated zones are significantly different than for samples from below the water table and from the near surface zone. Pyrite plus pyrrhotite account for about 80 wt % of the material in the sample at 3.0 m, for about 5 to 25 wt % in the unsaturated zone, and for less than 0.5 wt % near surface.

The pyrite-pyrrhotite-"goethtite+altered products ternary diagrams show the same trends for plus and for the minus 37 μm (400 mesh) fractions, but there is a better grouping for the plus 37 μm (400 mesh) fraction samples. It is noteworthy that Sample 3.0 m (No. 10) contains some goethite, and the pyrrhotite in the sample in partly altered. Furthermore, the position of the point for Sample 2.1 (No. 7) is between the position of the points for Samples 2.7 (No. 9) and 3.0 (No. 10), and the position of the point for Sample 2.4 (No. 8) is close to the water table boundary. This sequence for the samples from below the water table is the same as in the silicates-magnetite-pyrite+pyrrhotite ternary diagram. The points on the pyrite-pyrrhotite-"goethite"+altered products ternary diagram suggest that, below the water table, pyrrhotite alters at a faster rate than pyrite. Another observation is that the pyrite-pyrrhotite-goethite+ alteration products ternary shows a grouping of Samples 0.6 m to 1.8 m (No. 2-6) for the unsaturated zone rather than 0.9 to 1.8 (No. 3-6) as in the silicates-magnetite-pyrite+pyrrhotite ternary. This suggests that sample 0.6 is at the boundary between the saturated zone and a near surface zone. Sample 0.3 m which is from near surface, has a high "goethite" content and essentially no pyrite or pyrrhotite.

DISCUSSION

The mineralogical investigation has shown that (1) there is a progressive change in mineral quantities from the base to the surface of the tailings pile; (2) the tailings below the water table, in the unsaturated zone, and in the near surface zone have distinct mineralogical characteristics; and (3) alteration proceeds by transformation from pyrrhotite to an iron sulphate which in turn breaks down to a sulphur-rich "goethite", and by break down of pyrite to a low-sulphur "goethite". The amount of "goethite" in the tailings pile is relatively low which suggests that much of the iron and sulphur that were produced from the pyrite and pyrrhotite were probably washed away. It is possible, however, that some of the leached iron has remained and has been converted to magnetite.

The results given in Tables 3 and 4 indicate that (a) pyrite and pyrrhotite are essentially absent in the near surface zone; (b) about 10 to 30 per cent of the amount of pyrite and pyrrhotite assumed to have been present in the original tailings is still present in the unsaturated zone; and (c) about 1/2 the amount of pyrite and 1/4 the amount of pyrrhotite are still present just below the water table. It was also observed that the alteration bands on pyrrhotite are much wider in Samples 2.4 and 2.7 (2.4 to 2.7 m below the water table) than in Sample 3.0 (3.0 metres below the water table). These results suggest that decomposition of pyrite and pyrrhotite has been completed in the near surface zone, is progressing at a relatively high rate in the unsaturated zone, and at a slow rate below the water table. It is possible, however, that there is no decomposition of pyrite and pyrrhotite below the water table, but that, during the period from 1962 to 1985 the water table fluctuated between 2 and 3 metres below the surface of the tailings pile giving rise to the observed changes in mineralogical compositions below the present water table.

TABLE 1. Wt % of samples in sized fractions

Sample depth (m)	>37 µm fractions	<37 µm fractions	TOTAL
.30	93.98	6.62	100.00
.60	92.77	7.23	100.00
.90	92.10	7.90	100.00
1.20	96.52	3.48	100.00
1.50	94.33	5.67	100.00
1.80	94.05	5.95	100.00
2.10	93.26	6.74	100.00
2.40	94.47	5.53	100.00
2.70	85.08	14.92	100.00
3.00	92.14	7.86	100.00

TABLE 2. Quantitative EDXA analysis for minerals

Mineral	Sample	Fraction	Elements in wt %						Total
			Fe	S	K	Ca	Al	Si	
Pyrite	0.9m	>37 µm	47.0	54.3					101.3
Pyrite	1.2m	>37 µm	47.6	54.1					101.7
Pyrite	1.5m	>37 µm	47.7	53.5					101.2
Pyrite	1.8m	>37 µm	46.5	53.2					99.7
Pyrite	2.1m	>37 µm	47.0	54.3					101.3
Pyrite	2.1m	>37 µm	47.9	53.6					101.5
Pyrite	2.1m	>37 µm	45.6	53.1					98.7
Pyrite	2.4m	>37 µm	48.3	54.1					102.4
Pyrite	2.4m	>37 µm	47.0	53.5					100.5
Pyrite	2.7m	>37 µm	48.6	54.9					103.5
Pyrite	3.0m	>37 µm	47.9	55.0					102.9
Pyrite	3.0	<37 µm	47.3	54.8					102.1
Pyrrh.	0.9m	>37 µm	62.7	39.4					102.1
Pyrrh.	1.2m	>37 µm	61.6	39.4					101.1
Pyrrh.	1.2m	>37 µm	62.0	38.9					100.9
Pyrrh.	1.5m	>37 µm	62.2	37.8					100.0
Pyrrh.	2.4m	>37 µm	62.8	38.1					100.9
Pyrrh.	2.4m	>37 µm	59.8	38.5					98.3
Pyrrh.	2.7m	<37 µm	59.8	39.0					98.8
Pyrrh.	2.7m	<37 µm	57.9	40.9					98.8
Pyrrh.	3.0m	<37 µm	61.0	39.3					100.3
AP-type1	1.5m	>37 µm	42.6	54.1	-	0.2	-	0.1	97.1
AP-type2	1.5m	>37 µm	48.2	43.8	-	-	-	-	92.0
AP-type2	2.1m	>37 µm	42.7	50.2	-	-	-	-	92.9
AP-type2	2.7m	<37 µm	46.4	45.6	-	-	-	-	93.0
AP-type2	2.7m	<37 µm	41.8	48.4	-	-	-	-	90.2
AP-type2	2.7m	<37 µm	43.5	48.6	-	-	-	-	92.1
AP-type2	2.7m	<37 µm	43.0	48.0	-	-	-	-	91.0
AP-type2	ave.		44.3	47.4	-	-	-	-	91.7
AP-type3	1.8m	>37 µm	45.8	40.6	-	-	-	-	86.4
AP-type3	1.8m	>37 µm	42.8	42.4	-	-	-	0.3	85.5
AP-type3	2.7m	<37 µm	40.3	45.9	-	-	-	-	86.2
AP-type3	2.7m	<37 µm	40.0	46.0	-	-	-	-	86.0
AP-type3	ave.		42.2	43.7	-	-	-	0.1	86.0
AP-type4	1.5m	>37 µm	44.9	27.5	-	-	-		72.4
AP-type4	1.8m	>37 µm	41.6	37.8	-	-	0.3	0.2	79.9
AP-type4	2.1m	>37 µm	44.5	25.9	0.1	-	0.3	0.4	71.2
AP-type4	2.4m	>37 µm	44.5	27.0	-	-	0.1	0.2	71.8
AP-type4	2.4m	>37 µm	47.3	25.9	-	-	1.0	0.3	75.5
AP-type4	2.7m	>37 µm	44.1	34.4	-	0.2	0.1	0.2	79.0
AP-type4	2.7m	<37 µm	37.9	40.9	-	-	-	-	78.8
AP-type4	2.7m	<37 µm	42.4	16.7	-	-	-	-	60.1

AP = alteration product

AP-type4	2.7m	<37 µm	39.1	29.3	-	-	0.5	0.3	69.2
AP-type4	2.7m	<37 µm	42.3	16.6	-	-	-	-	58.9
AP-type4	2.7m	<37 µm	42.0	28.2	-	-	1.7	0.1	72.0
AP-type4	2.7m	<37 µm	40.2	32.3	-	-	-	-	72.5
AP-type4	ave.	<37 µm	42.6	28.6	-	-	0.3	0.1	71.6
AP-type?	2.4m	<37 µm	29.0	24.7	-	-	-	0.2	53.9
Goethite	0.6m	>37 µm	35.1	8.9	0.2	-	1.4	2.0	47.6
Goethite	0.9m	>37 µm	41.0	8.2	-	-	2.7	0.5	52.4
Goethite	0.9m	>37 µm	38.8	9.5	-	-	3.0	0.5	51.8
Goethite	0.9m	>37 µm	34.1	9.6	-	-	2.5	0.6	46.8
Goethite	0.9m	>37 µm	32.8	12.5	-	-	3.6	1.1	50.0
Goethite	1.2m	>37 µm	30.8	8.6	-	-	2.9	4.4	46.7
Goethite	1.2m	>37 µm	38.6	9.0	0.1	0.3	2.2	-	50.2
Goethite	1.2m	>37 µm	44.1	9.9	-	-	1.9	0.7	56.6
Goethite	2.1m	>37 µm	47.7	11.3	0.1	-	0.3	0.7	60.1
Goethite	2.4m	>37 µm	43.5	13.7	-	-	1.5	0.8	59.5
Goethite	2.7m	>37 µm	35.7	19.8	-	0.2	-	0.3	56.0
Goethite	3.0m	>37 µm	24.4	17.9	-	-	-	0.3	42.6
Goethite	2.7m	<37 µm	32.9	17.2	-	-	-	0.4	50.5
Goethite	2.4m	<37 µm	52.5	9.6	0.1	-	0.3	0.5	63.0
Goethite	ave.		38.0	11.8	-	-	1.6	0.9	52.3
Goethite	0.3m	>37 µm	52.8	2.4	-	-	-	0.5	55.7
Goethite	0.3m	>37 µm	54.3	2.0	0.2	-	0.2	0.6	57.3
Goethite	0.3m	>37 µm	50.2	5.1	0.7	-	0.3	0.9	57.1
Goethite	0.3m	>37 µm	52.6	2.5	-	-	-	0.5	55.6
Goethite	0.3m	>37 µm	48.6	5.1	0.8	-	0.5	0.8	55.8
Goethite	0.3m	>37 µm	45.3	1.1	-	-	-	5.4	51.8
Goethite	0.6m	>37 µm	50.3	1.6	0.1	-	0.4	3.2	55.6
Goethite	0.6m	>37 µm	53.8	2.6	0.1	-	0.5	0.5	57.5
Goethite	0.6m	>37 µm	46.0	2.8	-	-	0.2	0.9	49.9
Goethite	0.9m	>37 µm	49.8	4.6	-	-	1.2	0.6	56.2
Goethite	1.2m	>37 µm	42.4	5.2	-	-	3.3	0.3	51.2
Goethite	1.5m	>37 µm	48.8	5.0	-	-	2.4	0.5	56.7
Goethite	1.5m	>37 µm	47.6	2.1	0.1	-	0.5	2.0	52.3
Goethite	1.8m	>37 µm	49.0	3.3	0.1	-	0.1	0.3	52.8
Goethite	1.8m	>37 µm	41.6	4.7	0.1	-	0.5	0.5	47.4
Goethite	2.1m	>37 µm	53.1	4.5	-	-	0.2	0.8	58.6
Goethite	2.4m	>37 µm	46.5	2.0	0.1	0.3	1.5	4.1	54.5
Goethite	2.7m	>37 µm	48.5	1.7	-	0.2	0.6	2.5	53.5
Goethite	2.4m	<37 µm	50.2	4.9	-	0.3	1.2	0.6	57.2
Goethite	2.4m	<37 µm	46.7	1.8	-	-	1.2	0.8	50.5
Goethite	ave.		48.8	3.3	0.1	-	0.7	1.3	54.2
Jarosite	0.3m	>37 µm	26.6	10.5	3.8	-	-	0.6	41.5
Jarosite	1.8m	>37 µm	36.3	3.6	2.1	-	-	0.6	42.6

TABLE 3. Mineral quantities in >37 μm (+400 mesh) fractions

Mineral	Depth of Samples (metres)									
	0.3 wt %	0.6 wt %	0.9 wt %	1.2 wt %	1.5 wt %	1.8 wt %	2.1 wt %	2.4 wt %	2.7 wt %	3.0 wt %
Quartz	27.4	37.5	56.5	41.4	12.6	34.3	14.4	19.3	26.1	7.2
Orthoclase	6.9	10.3	9.2	11.0	4.9	14.9	2.5	8.5	6.4	2.0
Chlorite	1.7	1.6	4.3	7.0	2.7	7.4	2.3	6.2	3.9	1.3
Amph.+pyrox.	2.5	1.8	6.4	7.1	1.8	7.0	2.3	6.1	3.3	0.8
Goethite	14.2	1.4	5.1	8.1	5.8	7.3	2.8	6.3	3.1	1.1
Pyrite	0.3	2.1	5.4	2.9	3.5	5.9	45.5	25.5	21.4	62.5
Magnetite/ hematite	46.8	43.6	10.4	13.5	37.9	7.5	12.7	19.4	18.6	7.5
Altered pyrr.	0.0	0.1	0.4	2.0	12.2	7.3	5.8	5.1	2.9	2.4
Pyrrhotite	0.0	0.1	1.1	5.9	17.2	6.5	10.8	3.0	13.7	14.1
Chalcopy+sph.	0.0	1.3	1.0	1.1	0.5	1.9	0.7	0.5	0.6	1.1
Arsenopy+tet.	-	-	-	-	0.1	-	-	-	-	-
Gal.+cass.	0.1	0.2	0.2	0.0	0.7	0.0	0.2	0.1	0.1	0.0
Goeth. on sil.	0.7	0.5	0.8	1.0	0.5	1.0	0.3	1.1	0.5	0.2
Goeth. on mag.	1.1	0.2	0.1	0.6	0.8	0.6	0.2	0.5	0.2	0.1
Goeth. on pyr.	0.0	0.0	0.1	0.2	0.4	0.9	0.5	0.5	0.3	0.1

TABLE 4. Mineral quantities in <37 μm (-400 mesh) fractions

Mineral	Depth of Samples (metres)									
	0.3 wt %	0.6 wt %	0.9 wt %	1.2 wt %	1.5 wt %	1.8 wt %	2.1 wt %	2.4 wt %	2.7 wt %	3.0 wt %
Quartz	19.6	19.3	32.4	12.5	18.2	12.4	14.0	12.1	22.0	8.3
Orthoclase	10.5	8.7	13.3	5.8	8.9	7.0	4.4	7.2	7.0	3.6
Chlorite	1.7	1.8	5.7	3.8	2.9	2.4	3.4	2.7	3.2	2.1
Amph.+pyrox.	3.1	7.5	12.9	15.4	8.0	11.0	8.7	8.2	8.4	3.8
Goethite	32.2	14.7	12.7	35.6	24.1	38.6	13.8	18.1	10.6	2.8
Pyrite	0.0	4.0	5.1	4.4	5.5	7.0	30.8	20.1	14.4	53.2
Magnetite/ hematite	33.8	41.4	14.2	14.7	21.3	15.4	18.3	20.8	14.3	8.7
Altered pyrr.	0.2	0.1	0.4	2.3	6.6	2.8	6.6	7.7	4.7	3.8
Pyrrhotite	0.2	0.2	1.9	4.3	4.2	1.6	4.2	2.7	14.1	11.6
Chalcopy+sph.	0.0	2.3	0.4	1.1	0.1	1.0	1.4	0.4	1.1	1.2
Arsenopy+tet.	-	-	0.3	-	-	-	-	-	-	0.1
Gal.+cass.	0.7	0.1	0.8	0.1	0.2	0.7	0.4	0.1	0.2	0.8

*magnetite could include hematite; pyrr. = pyrrhotite; sph. = sphalerite; tet. = tetrahedrite; gal. = galena; cass. = cassiterite; goeth. = "goethite"; sil. = silicates; mag. = magnetite; pyr. = pyrite

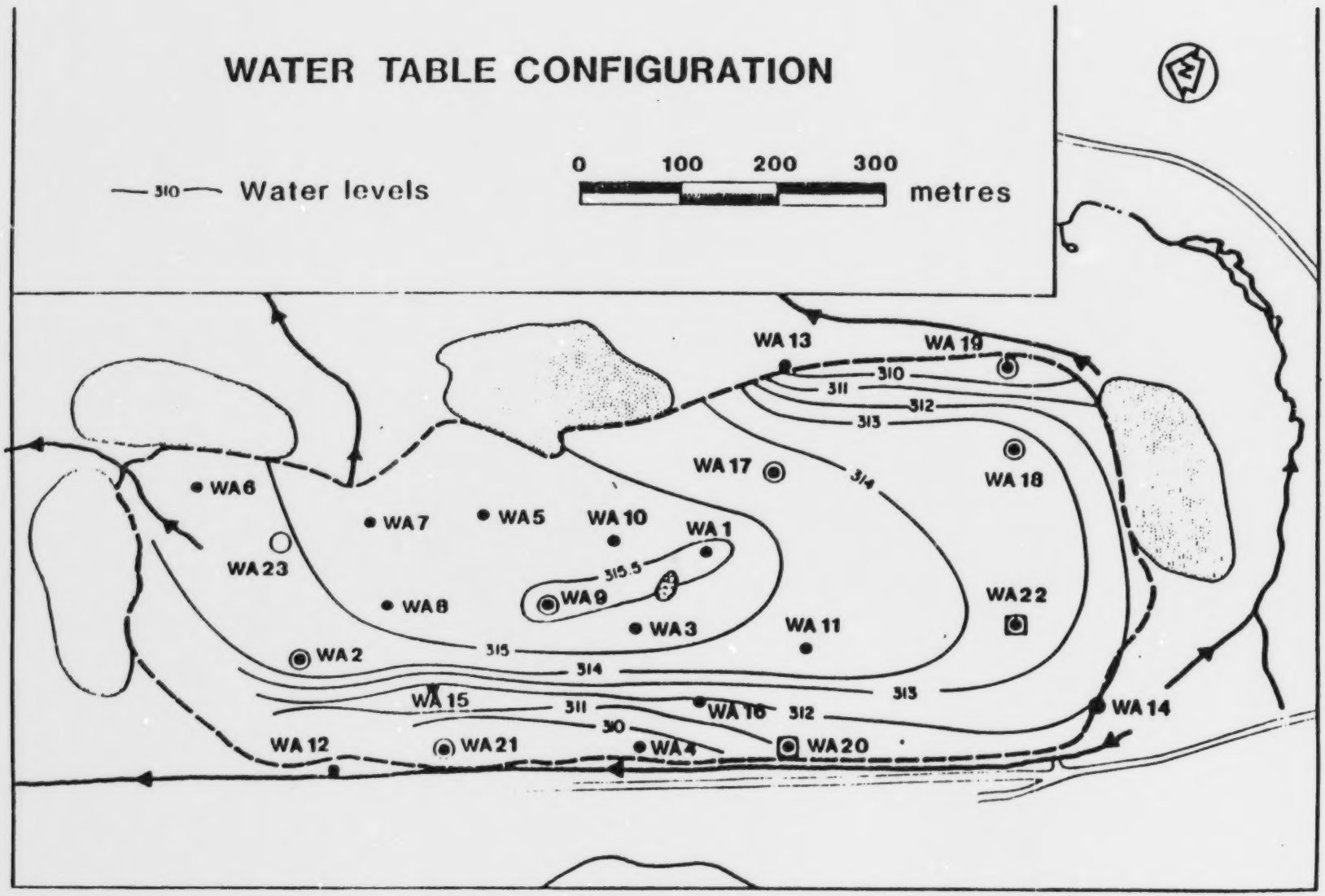

Fig. 1. Plan of Waite Amulet Tailings pile showing locations of piezometer nests, drill core sites, and water table horizons (from report submitted by Noranda Mines)

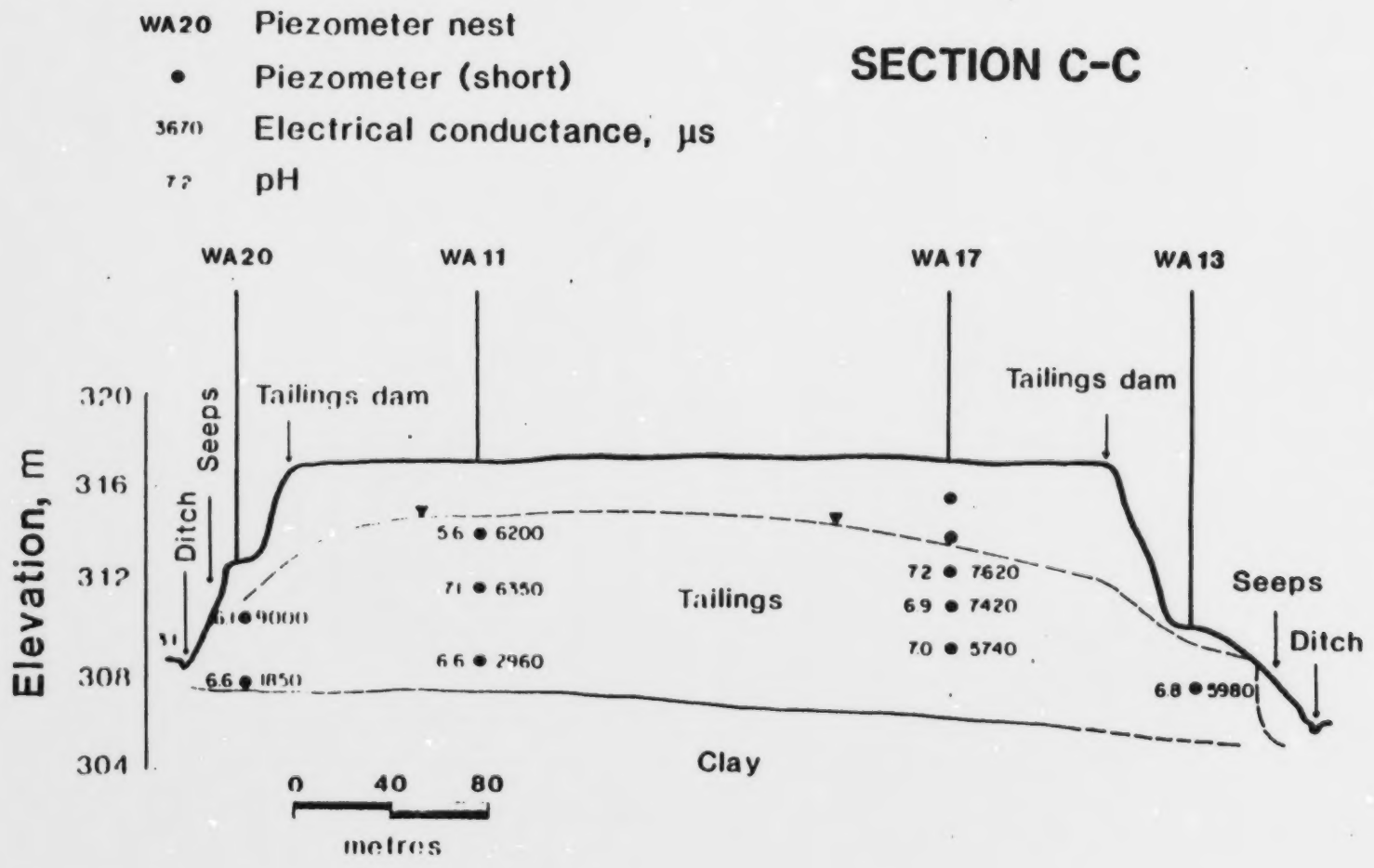

Fig. 2. Cross-section of Waite Amulet tailings pile showing location of drill core WA20 (from report submitted by Noranda Mines)

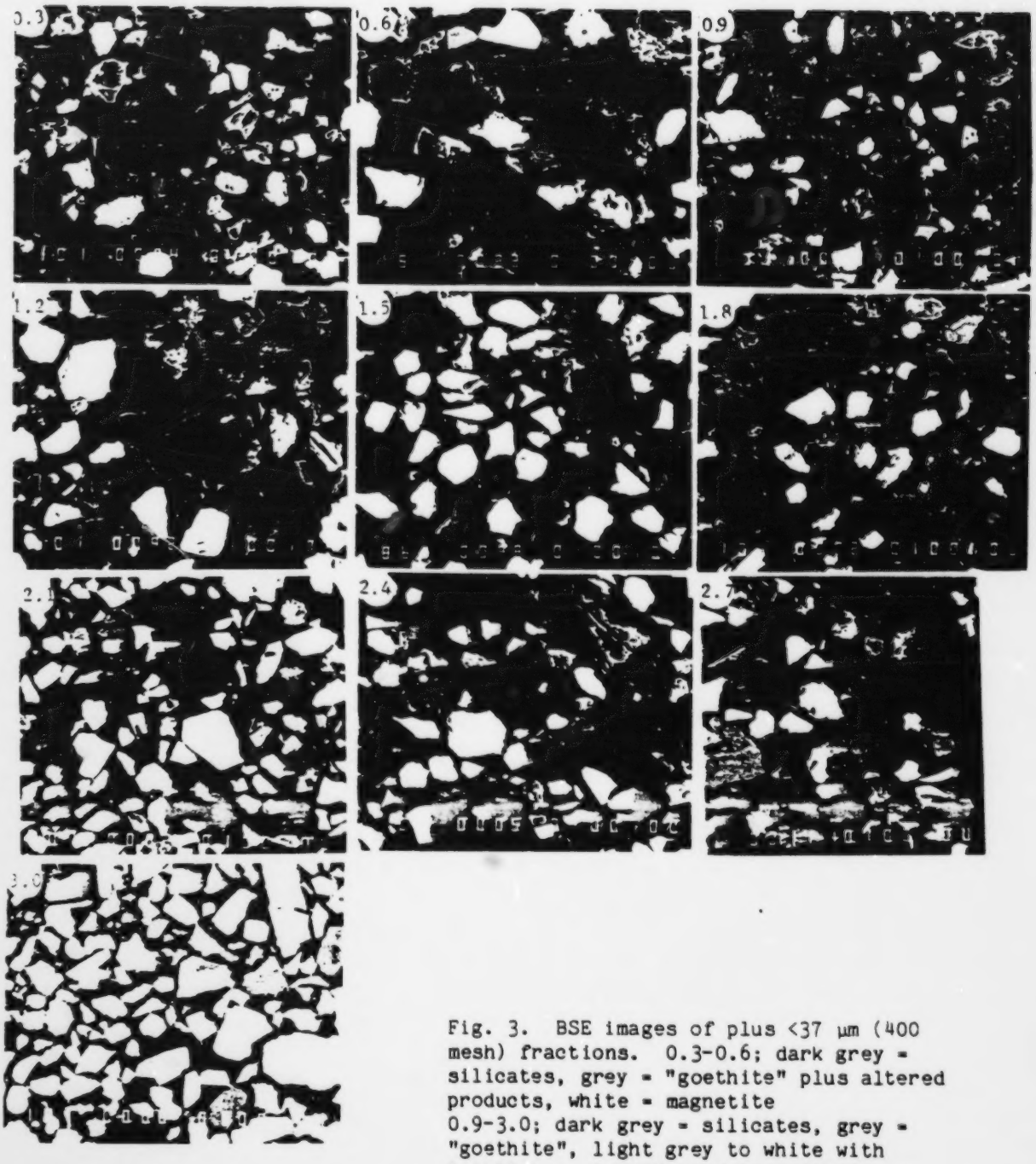

Fig. 3. BSE images of plus <37 μm (400 mesh) fractions. 0.3-0.6; dark grey = silicates, grey = "goethite" plus altered products, white = magnetite
0.9-3.0; dark grey = silicates, grey = "goethite", light grey to white with lamellae = altered products, white = pyrite, pyrrhotite and magnetite

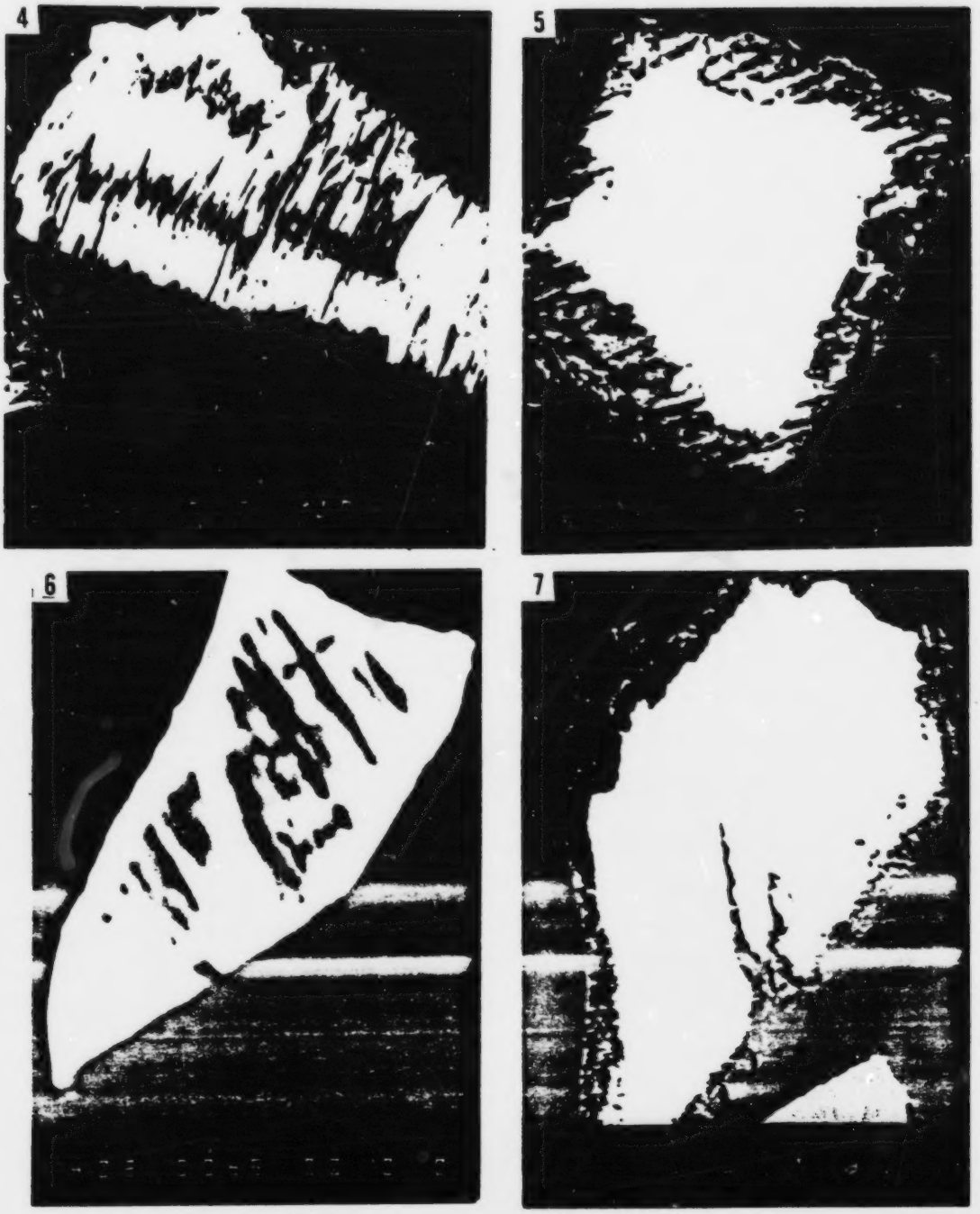

Fig. 4. BSE image showing pyrrhotite (white) surrounded by phase 1 alteration product.

Fig. 5. BSE image showing pyrrhotite (white) surrounded by phase 2 alteration product.

Fig. 6. BSE image of an alteration product (phase 3) showing lamellae that are assumed to be $FeSO_4$.

Fig. 7. BSE image showing pyrrhotite (white) bordered by phase 4 alteration product.

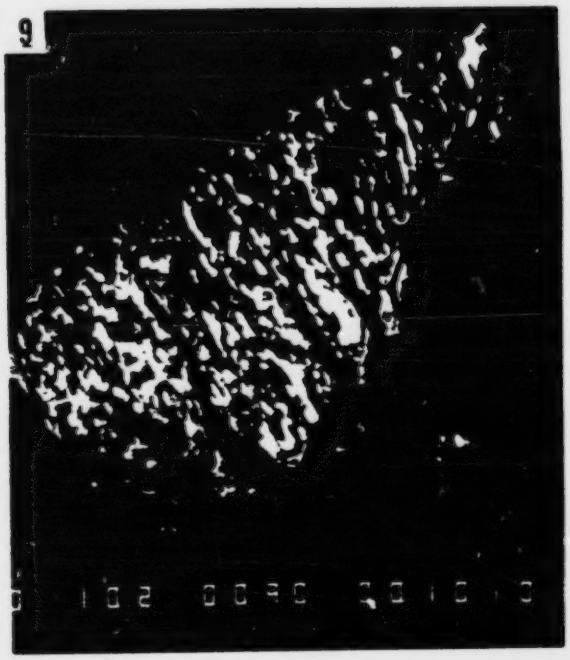

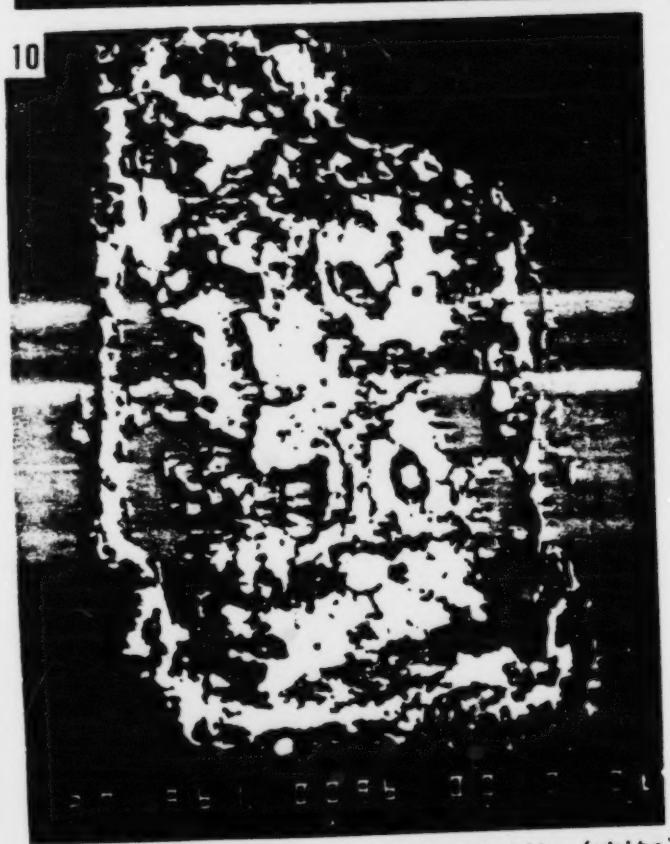

Fig. 8. BSE image showing pyrrhotite (white) partly replaced by alteration products.
Fig. 9 BSE image showing pyrrhotite nearly replaced by an alteration product.
Fig. 10. Pyrite remnants in "goethite".

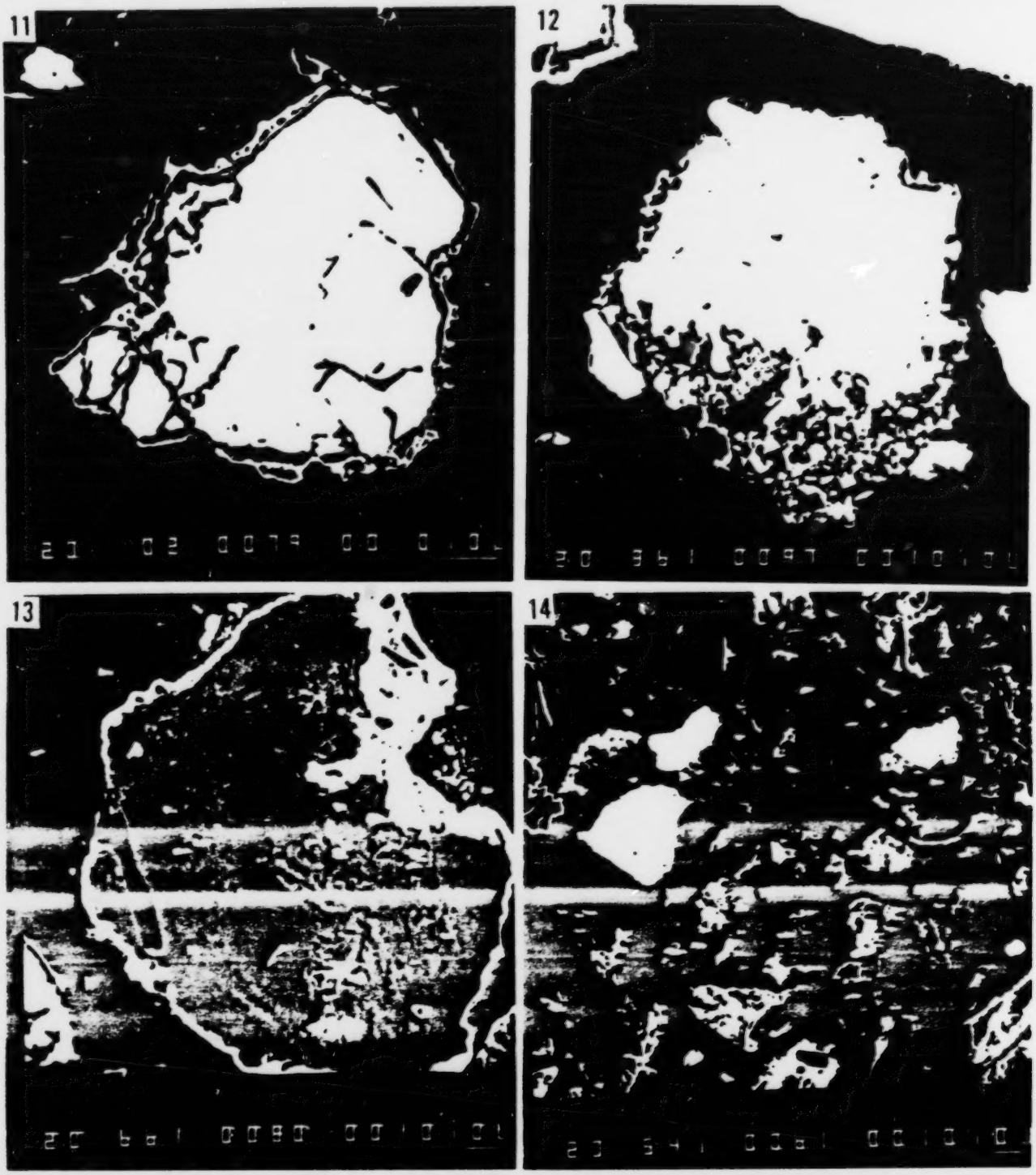

Fig. 11. BSE image showing a magnetite grain bordered by a low-sulphur "goethite".
Fig. 12. BSE image showing a magnetite grain bordered by a sulphur-rich "goethite". The magnetite in the lower part of the diagram appears to have been partly replaced by the "goethite".
Fig. 13. BSE image showing a quartz grain bordered by "goethite".
Fig. 14. BSE image of the sample at 0.3 m (near surface) showing discrete grains of "goethite" (grey) and magnetite (white).

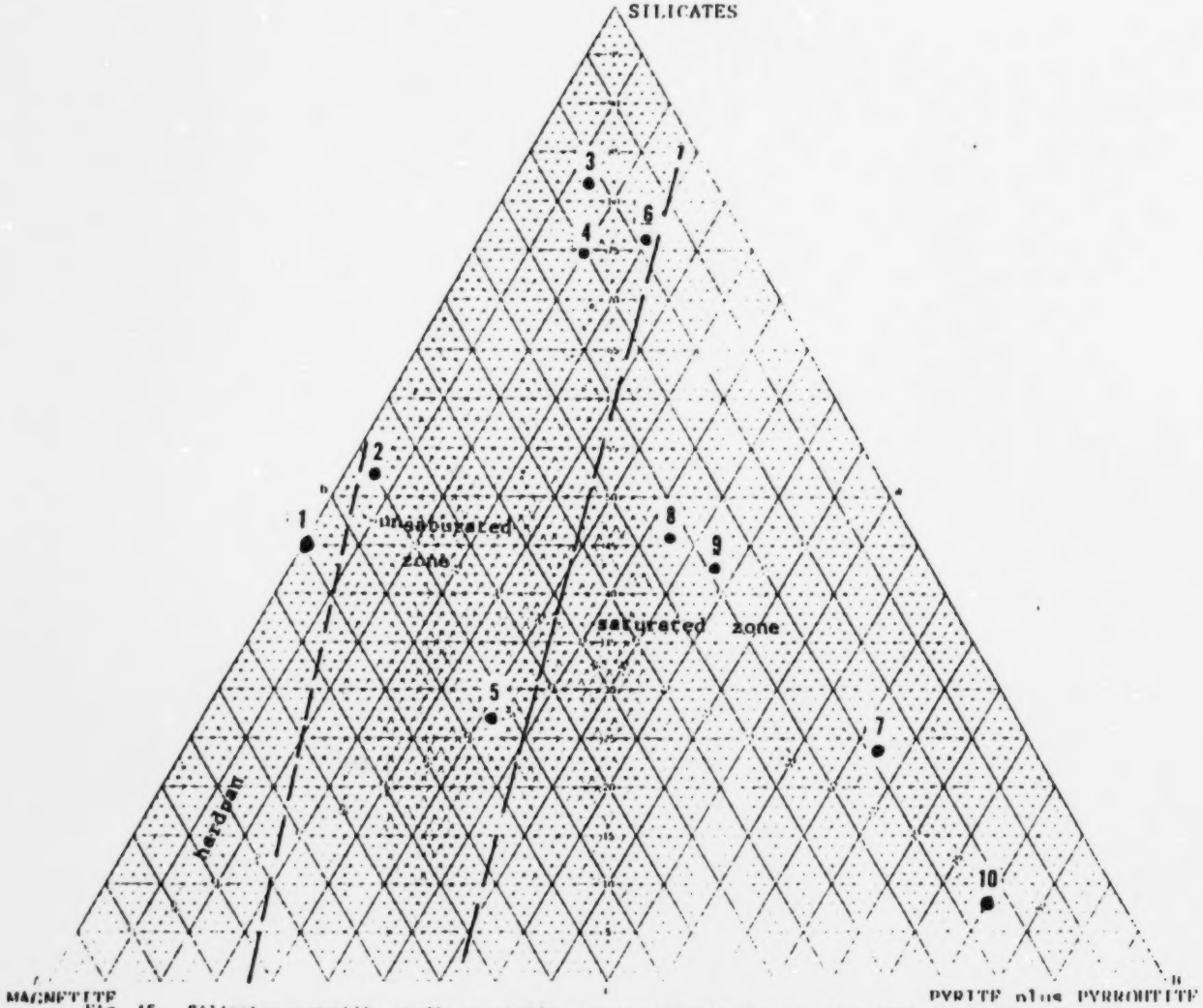

Fig. 15. Silicates-magnetite-pyrite+pyrrhotite ternary diagram for the plus (400 mesh) >37 μm fractions. 1 = 0.3 m, 2 = 0.6 m, 3 = 0.9 m, 4 = 1.2 m, 5 = 1.5 m, 6 = 1.8 m, 7 = 2.1 m, 8 = 2.4 m, 9 = 2.7 m, 10 = 3.0 m.

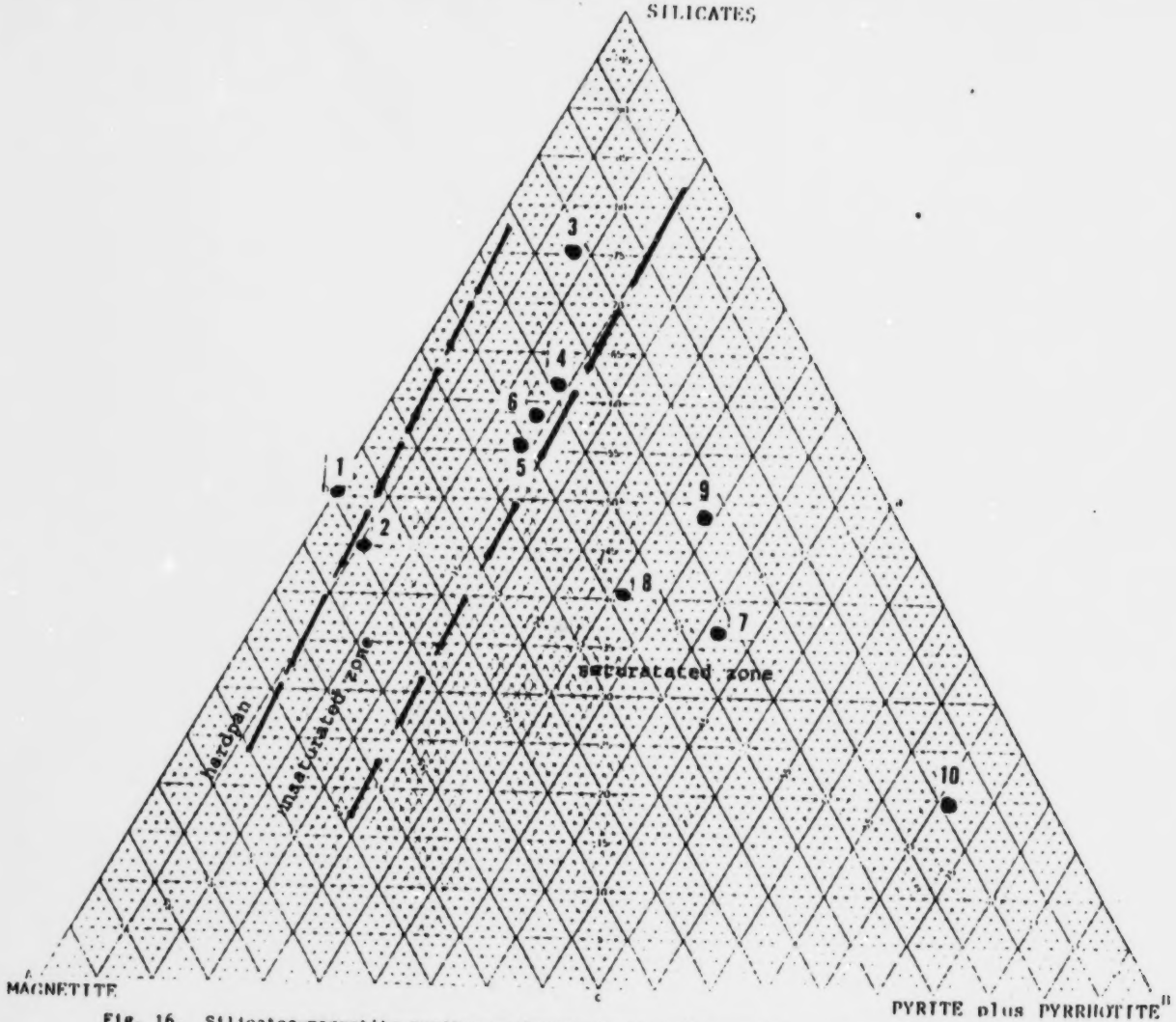

Fig. 16. Silicates-magnetite-pyrite+pyrrhotite ternary diagram for the minus <37 μm (400 mesh) fractions. 1 = 0.3 m, 2 = 0.6 m, 3 = 0.9 m, 4 = 1.2 m, 5 = 1.5 m, 6 = 1.8 m, 7 = 2.1 m, 8 = 2.4 m, 9 = 2.7 m, 10 = 3.0 m.

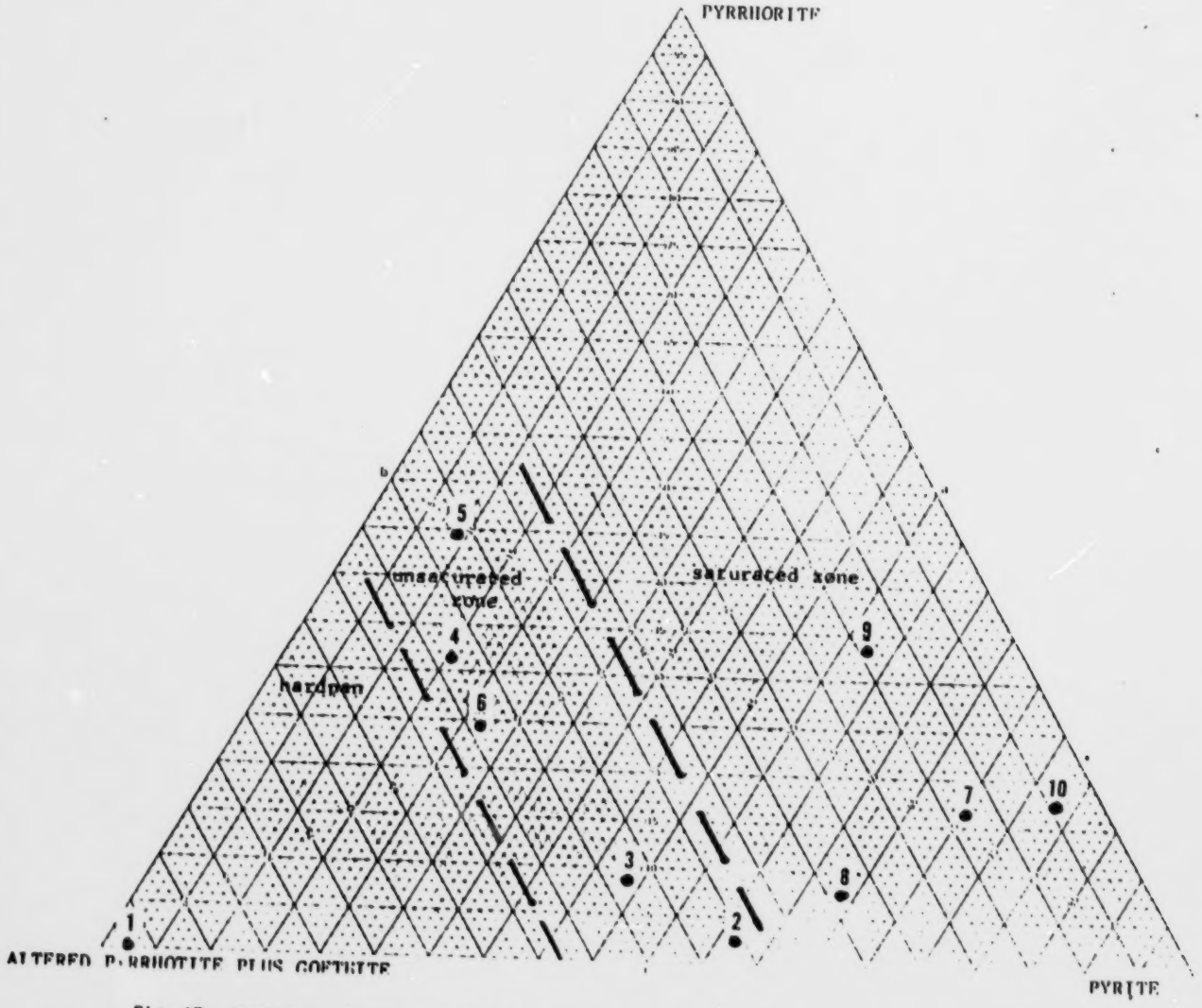

Fig. 17. Pyrite-pyrrhotite-goethite + alteration products ternary diagram for >37 μm (plus 400 mesh) fractions. 1 = 0.3 m, 2 = 0.6 m, 3 = 0.9 m, 4 = 1.2 m, 5 = 1.5 m, 6 = 1.8 m, 7 = 2.1 m, 8 = 2.4 m, 9 = 2.7 m, 10 = 3.0 m.

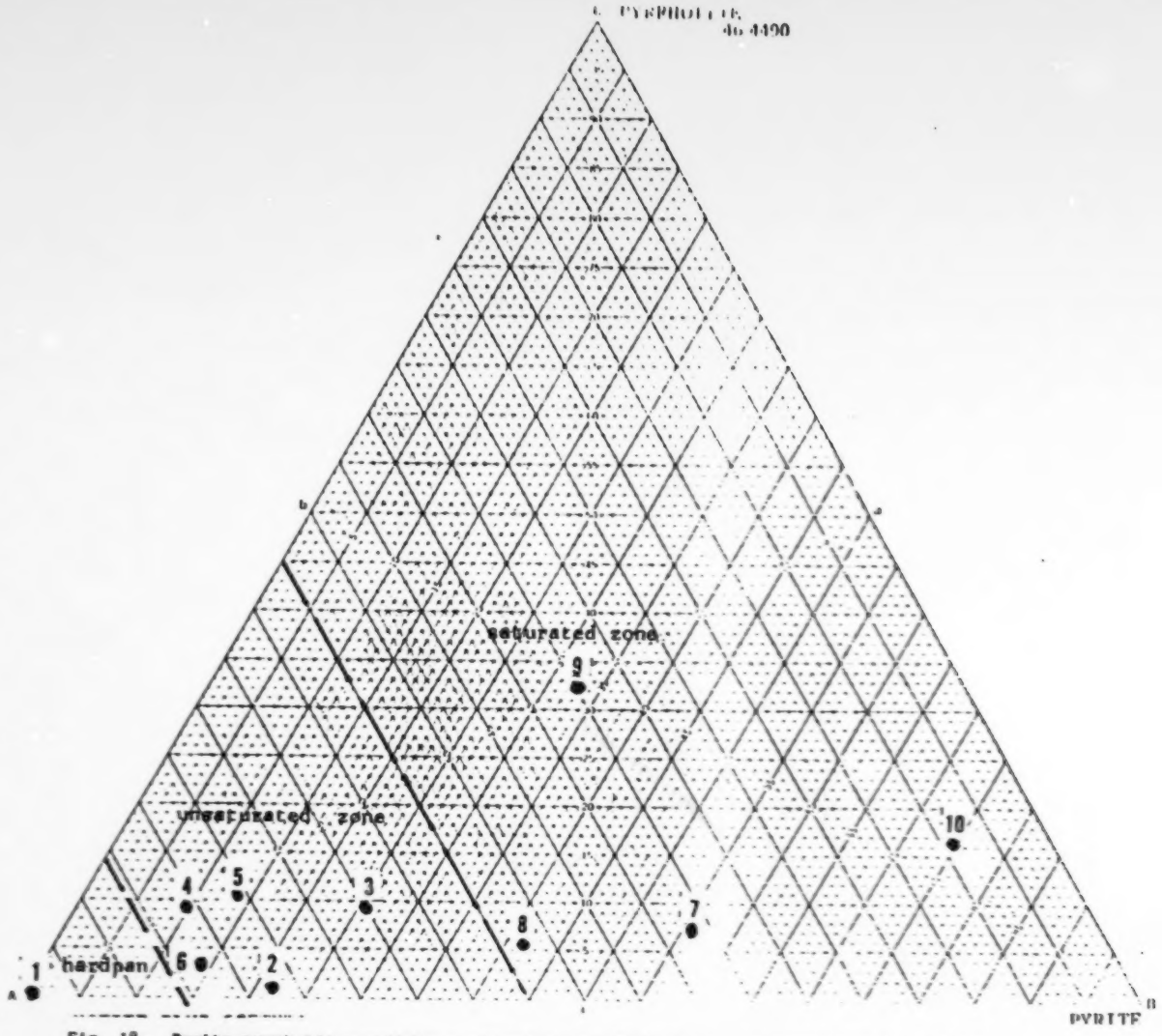

Fig. 18. Pyrite-pyrrhotite-goethite + alteration products ternary diagram for the <37 μm (minus 400 mesh) fractions. 1 = 0.3 m, 2 = 0.6 m, 3 = 0.9 m, 4 = 1.2 m, 5 = 1.5 m, 6 = 1.8 m, 7 = 2.1 m, 8 = 2.4 m, 9 = 2.7 m, 10 = 3.0 m.